

## A fast Hough transform for inspecting accurate needle-type meter gauges

Ke-qing Li\* and Qi Tian  
 Computer Vision Laboratory, Computer Center  
 \*Dept. of Information System and Engineering  
 Taiyuan University of Technology  
 Taiyuan, Shanxi, 030024, P.R.China

## ABSTRACT

A fast Hough transform (FHT) is presented in this paper for inspecting the accuracy of needle-type meter gauges with up to 0.2% relative accuracy. The number of computations to implement this algorithm is less than one thousandth of the number for the common HT. The proposed fast HT is based on a shape analysis of the HT surface  $Z(\rho, \alpha)$  for the needle of instruments and the nature of the inspection. Experiments show that the surface around peaks is a quasi-singly peaked smooth surface. Considering that property of the surfaces, and that the needle is staying around a set of predetermined angles,  $\alpha_k$ , therefore, we can perform the HT only for parameter  $\alpha$  within  $\alpha_k \pm \delta\alpha$  instead of whole range of  $\alpha$ , 0-180°. The former is only about one hundredth of the latter. The shape analysis of the surface  $Z(\rho, \alpha)$  around peak positions is useful in other applications as well. Theoretical analysis and experimental results show that by properly choosing the spatial resolution of the digitization,  $M$ , and the HT parameter angular resolution,  $\Delta\alpha$ , meter gauges of different accuracy grades can be automatically inspected. For example, in order to inspect instruments with 0.2% accuracy, a 512×512 image and  $\Delta\alpha = 0.2^\circ$  should be used.

## 1. Introduction

In massive productions of various needle-type meter gauges, traditional manual procedures to inspect gauges hardly meet the speed and accuracy requirements. In 1982, Baird suggested an automatic inspection system, GAGESIGHT, which can be used to verify if the rest position of needles is correct with respect to the markings on the face of the gauges[1]. In 1983, Dyer proposed another system for verifying accuracy of the needle positions on a gauge for a set of analog inputs [2]. In this paper, based on a shape analysis of the Hough surface, a fast Hough transform (FHT) is presented for inspecting needle-type gauges. In Section 2, a brief review of inspection principles is presented and factors limiting the inspection accuracy are analyzed. In Section 3, we will examine inherent noise in the Hough domain and study shapes of the Hough surface and projection areas of Hough surfaces on the  $(\rho, \alpha)$  plane. Section 4 describes the FHT algorithm and some experimental results. Conclusions are presented in Section 5.

## 2. Principles of inspections

The basic procedures for inspecting needle-type gauges are as follow: (1) applying a set of specified analog inputs to a meter, digitize images of the meter gauge while the needle is in corresponding rotated positions; (2) compute difference images between pairs of digitized images, properly binarizing the images; (3) perform the HT and determine if the relative angular displacements of the nee-

dle are within the accuracy specification of the instrument. The advantages of using the HT to measure the angular displacements of needles is that the HT is not sensitive to noises of digitized images and breakpoints on lines to be detected.

For simplicity and easy observation, we will use the modified normal parameters  $(\rho, \alpha)$  instead of the parameters  $(\rho, \theta)$ ,

$$\rho = \text{Sign}(\alpha - 90)(X \text{Sin}\alpha - Y \text{Cos}\alpha) \quad (1)$$

where  $\alpha$  is the slope angle of the needle as indicated in Fig. 1. Now, we will investigate the factors which affect inspection accuracy  $\varepsilon_0$ , spatial resolution of images,  $M$ , the sampling rate of the parameter  $\alpha$ ,  $\Delta\alpha$ . Because images of needle-type meter are spatially digitized with a limited dimension,  $M$ , and the parameter  $\alpha$  of the HT is sampled with a certain resolution  $\Delta\alpha$  as well, there is a minimum angle,  $\varepsilon_0$ , of the needle displacements, which the inspection system can measure. Suppose that in a digitized image a needle is of  $L$  pixels, and it is rotated by a small angle  $\phi$ , if the end point has been moved away from the original position by 1 pixel, then it is possible to use the HT to detect this rotation. Values of  $\phi$  depend on the initial slope of the needle, but it can be easily shown that, at an extreme,  $\phi \geq \arctg \frac{1}{L}$ . As indicated in Fig. 1, if the needle has a maximum pixel length  $L$ , the spatial resolution is  $M \times M$  and the maximum rotation angle of the needle from the rest position to the full scale position is denoted by  $\delta_{max}$ , then, at least,  $M \times M$  digitized images will provide a minimum detectable angle

$$\phi = \arctg \frac{1}{L} = \arctg \left[ \frac{2 \text{Cos}(\frac{180 - \delta_{max}}{2})}{M} \right] = \arctg \left[ \frac{2}{M} \text{Sin}(\frac{\delta_{max}}{2}) \right]$$

Moreover, in order to detect the angle difference  $\phi$ , the sampling resolution of the HT parameter  $\alpha$ ,  $\Delta\alpha$  has to be chosen properly. If  $\Delta\alpha$  is too small, this high resolution is wasted since at the first place digitized images does not provide a compatible high resolution, on the other hand, if it is chosen too large, the high spatial resolution of images is wasted. Thus, in general, we will choose  $\Delta\alpha \approx 1.0 \sim 2.0\phi$  since in image digitization, we may not take the full resolution of images, meter needles may only takes part of images. Thus, in general, we will have

$$\varepsilon_0 \geq \Delta\alpha \geq \phi = \arctg \left[ \frac{2 \text{Sin}(\frac{\delta_{max}}{2})}{M} \right] \quad (2)$$

For examples, for meters with  $\delta_{max} = 100^\circ$ , using different sampling rate,  $M=256, 512, 1024$ , from Eq. (2),  $\phi$  can be calculated as  $0.35^\circ, 0.2^\circ, 0.085^\circ$ , then  $\Delta\alpha$  can be chosen as  $0.5^\circ, 0.2^\circ, 0.1^\circ$ , respectively, corresponding inspection accuracy  $\varepsilon_0$  are  $0.5^\circ, 0.2^\circ$ ,

0.1° accordingly.

Moreover, for different meters widths of needles are different. In our experiments we have tested our algorithm for needles with different widths, 1-5 pixels, results show that variations of the needle width does not affect inspection accuracy of the needle angle. It is because a wider needle can be considered as a set of parallel lines with the same slope angle, after the HT they have the same  $\alpha$ , and different  $\rho$ . Therefore, in a certain extent, the inspection accuracy is not affected by the width of needles.

### 3. Analysis of the Hough surfaces

In this Section, we will study the natures of the Hough surface and show that great savings in computations can be achieved by using the proposed FHT.

In general, an accumulator array  $Z(\rho, \alpha)$  for the HT defines a surface in the three dimensional space  $(Z, \rho, \alpha)$ . Procedures of performing a HT can be divided into two steps: calculating  $Z(\rho, \alpha)$  over a range of the parameters  $(\rho, \alpha)$  for a given image and finding some peak values of the surface  $Z(\rho, \alpha)$ , which correspond to some straight lines in the given image. Theoretically, a straight line in the image domain corresponds to a point  $(\rho_0, \alpha_0)$  in the Hough domain. But, in the digital implementation of the HT, lines are digitized with a limited resolution, therefore, a line corresponds to a Hough surface  $Z(\rho, \alpha)$ , which has a peak at the point  $(\rho_0, \alpha_0)$ , and it decreases quickly while  $(\rho, \alpha)$  is away from the peak position  $(\rho_0, \alpha_0)$ . Studying approximate locations and shape of the Hough surface, we can save computations in two ways: first, if the approximate locations of peaks can be estimated with certain tolerance, then we can perform HT only for these limited regions instead of the whole range of the  $\rho$  and  $\alpha$ ; second, if we know more about the surface shape locating peak positions can be performed more efficiently by using heuristic search procedures, instead of using blind exhausted search.

Now, we will show that by using exhausted searching it is not easy to locate correct peak positions of  $Z(\rho, \alpha)$ . We have digitally created a binary image with a dimension  $256 \times 256$ , there are two straight lines,  $\alpha_1 = 40^\circ$ ,  $\alpha_2 = 90^\circ$ . For the HT parameter we choose  $\Delta\alpha = 0.5^\circ$ ,  $\Delta\rho = 1$  pixel. After performing HT, the first eight largest values of  $Z(\rho, \alpha)$  are listed in Table 1. It can be seen that the first three values came from line 2; the fourth and the fifth values from line 1. Because line 1 is in a diagonal direction so that its maximum value, 120, is smaller than the maximum value, 167, of line 2. In this Table only the first and fourth entries correspond to the lines in the given image, others are caused by digitization, we will call them inherent noises for the HT. As illustrated above, exhausted search hardly locates local peaks of  $Z(\rho, \alpha)$ . Because of the existence of the inherent noises, finer quantization of the Hough parameter  $\alpha$  makes the situation worse. If  $\alpha$  is sampled too coarse, i.e.,  $\Delta\alpha$  increases, then the minimum angle,  $\epsilon_0$ , which the inspection system can detect, is increased. In our experiments, a  $Z(\rho, \alpha)$  is calculated for a difference image with a needle in two positions:  $\alpha_1 = 60^\circ$  and  $\alpha_2 = 120^\circ$ , and it is printed in Fig. 2 where lower values are represented by coarser black dots, higher values by denser black dots, there are total eight grey levels. Because we have chosen the origin of the image coordinates  $(x, y)$  near the rotation axle of the needle so that peaks are located on areas where

$\rho \approx 0$ . Analysis shows that when a needle is at different angles, the peak of  $Z(\rho, \alpha)$  changes its location along the  $\alpha$ -axis, but the shape of the  $Z(\rho, \alpha)$  around a small neighborhood centered at a peak  $(\rho_0, \alpha_0)$  does not change. Given a threshold value  $C_t$ , all points around  $(\rho_0, \alpha_0)$  which satisfy  $Z(\rho, \alpha) \geq C_t Z(\rho_0, \alpha_0)$  constitute a set  $S$ ,  $S$  has a shape of two identical right triangles as illustrated in Fig. 3. A three dimensional  $Z(\rho, \alpha)$  surface is plotted in Fig. 4, in a logarithm  $Z$  scale to show the peak's shape more clear. The plotting indicates that the surface around the peak is a quasi-singly peaked smooth surface. The position of the peak corresponds to the needle slope, its height represents the length of the needle in pixels.

In [4], we have shown that if a needle has a length  $L$  pixels, and given the threshold value  $C_t$ , then the set  $S$  defined above can be determined as follow:

$$\delta\alpha_{max} = \frac{57.3}{C_t L} \quad (3)$$

$$\delta\rho_{max} = \frac{3|0.5 - C_t|}{C_t} \quad (4)$$

These Equations have been verified with an experiment where an image with a straight line,  $\alpha = 120^\circ$ ,  $L = 146$  pixels, which goes through the  $(x, y)$  origin, was Hough-transformed using parameters  $\Delta\rho = 1$ ,  $\Delta\alpha = 0.5^\circ$ , the resulted  $Z(\rho, \alpha)$  is represented in Fig. 3. From Eq. (3) and (4),  $\delta\rho_{max} = 27$  pixels and  $\delta\alpha_{max} = 7.85^\circ$ , these results are coincident with the experimental results well. As stated early, for the difference image of needles, its Hough surface consists of two similar quasi-singly peaked surfaces, they are apart from each other by an angle  $\phi$  along the  $\alpha$ -axis. If we choose a proper plane,  $Z = C_t$ , to intercept the surface  $Z(\rho, \alpha)$ , as long as a  $\delta\alpha_{max}$ , calculated from Eq. (3), is smaller than a half of the angle between the needle's two positions, then the intercepted surfaces are two separated quasi-singly peaked surfaces, their projections onto the plane  $(\rho, \alpha)$  are two separated twin right triangle areas. Thus, we can perform the HT only over these two small areas, and search for two local peaks, respectively.

Now, let's estimate by using this method, in terms of computations how much savings can be achieved. Because the HT is performed over two smaller areas,  $D_1$  and  $D_2$ , instead of whole plane  $(\rho, \alpha)$  it requires much less computations than the common HT. For an example, a given image with a resolution  $256 \times 256$  has  $K$  pixels of nonzero values, to perform the common HT over the whole plane  $(\rho, \alpha)$ ,  $-128 \leq \rho \leq 128$  and  $0^\circ \leq \alpha \leq 180^\circ$ , using sampling rates  $\Delta\alpha = 0.5^\circ$ ,  $\Delta\rho = 1$  pixel, needs  $K \times 360 \times 256 = 92160K$  point operations (each point operation requires one addition and two multiplications). On the other end, using the proposed algorithm, for  $L = 167$  pixels,  $C_t = 0.2$ , from Eq. (3),  $\delta\alpha_{max} = 2^\circ$ ,  $\delta\rho_{max} = 4.5$ . As we will explain in the next Section, by properly choosing the origin of the digitized images, the search region for  $\rho$  can be limited in a region  $|\rho| \leq 3$  pixels, then to perform the HT over these regions only needs  $\frac{K \delta\alpha_{max}}{\Delta\alpha} \times \frac{6}{\Delta\rho} = 48K$  point operations, it is less than one thousandth of the original computation, 92160K. Similarly, searching over the whole  $(\rho, \alpha)$  plane requires 92160 comparisons, but, based on the quasi-singly peaked property of the HT surface, using heuristic search algorithms, such as hill-climbing, in an average, only needs  $\frac{1}{3} \times 48$  comparisons. In comparison with the common HT, in terms of computations and

memory storages, the proposed fast Hough transform provides savings in computations more than several hundreds times.

#### 4. The Fast Hough transform

Now, we are going to formalize the Fast Hough transform for the inspection of needle-type meters. Based on the above analyses, it is obvious that if we can choose a proper threshold  $C_t$  for the given set of analog inputs of meters to ensure that the angle between two needle positions,  $\beta$ , is larger than  $2\delta\alpha_{max}$ , where  $\delta\alpha_{max}$  is determined by Eq. (3), then, the corresponding Hough surface is intercepted into two separated quasi-singly peaked surfaces by the plane  $Z = C_t$ . Thus, according to the ranges of given inputs and the  $\delta\alpha_{max}$  value the two small regions in the H domain can be determined. Therefore, the two peaks of the HT corresponding to the two needle's positions are located in these two separated regions. The accurate positions of the two peaks can be determined by searching through these two regions, respectively. In addition, there is no need to calculate the HT over the full range of parameter space, instead, it is only necessary to perform HT over the two small regions. The FHT can be summarized as follow:

- (1). According to the accuracy specification, and  $\delta_{max}$  of the meter, choose  $\varepsilon_0 = 0.5$  and then from Eq. (2) determine a proper spatial resolution  $M$  to digitize meter images, and a sampling rate,  $\Delta\alpha$ , of the Hough parameter  $\alpha$ .
- (2). For each type of meters, construct a table which consists of three columns; input analog values, corresponding angular tolerance values of the angles for each input according to the accuracy specification, and test results.
- (3). Applying a set of  $N+1$  predetermined analog inputs to the meter, inclusive of zero input, digitize  $N+1$  frame images of the meter face;  $I_0$  to  $I_n$ , for the needle at different angles from the rest position to the full scale position. During digitizing illumination and camera geometric position should not be changed.
- (4). Initially,  $i = 1$ , Calculating a difference image  $\Delta I_i = |I_i - I_0|$ , we choose  $90\%I_h$  as a threshold value to binarize the difference image  $\Delta I_i$  where  $I_h$  is the peak intensity of the histogram of the image  $\Delta I_i$ .
- (5). Properly choose the origin of the  $(x,y)$  coordinate so that the rotation axle of the needle is near the  $(x,y)$  origin, then the HT can be performed only for  $|\rho| \leq R$ ,  $R$  is in a range of 3 to 8 pixels depending on the image sampling rate. Determine the region  $D_1$  which corresponds to the needle in the rest position:  $-3 \leq \rho \leq 3$  pixels,  $\alpha_0 - \delta\alpha_{max} \leq \alpha \leq \alpha_0 + \delta\alpha_{max}$ , where  $\alpha_0$  is the angle of the needle in the rest position and  $\delta\alpha_{max}$  is calculated from Eq. (3); perform the HT over  $D_1$  region using  $\Delta\rho = 1$  pixel and  $\Delta\alpha = \varepsilon_0$ , and search the local peak over  $D_1$  region to find the angle  $\phi_0$  of the needle in the rest position.
- (6). Determine the region  $D_2$  corresponding to the needle for a nonzero input  $V_i$ :  $-3 \leq \rho \leq 3$  pixels and  $\alpha_i - \delta\alpha_{max} \leq \alpha \leq \alpha_i + \delta\alpha_{max}$ , where  $\alpha_i = \alpha_0 + \delta(V_i)$ . Perform the HT and searching to obtain the angle  $\phi_i$ .
- (7). Verify if the angle  $\beta_i = |\phi_i - \phi_0|$  is within the tolerance range of the meter:  $[\delta(V_i) - \varepsilon, \delta(V_i) + \varepsilon]$ . If it is inside this range

this meter satisfies the given accuracy specification for this input; otherwise, it is out of accuracy tolerance range, the meter fails.

- (8). Increasing  $i$  by 1, repeat the procedures 4 through 7. If the all  $N$  difference images all pass the inspection, it means that the meter succeeds the accuracy testing. Otherwise, it fails. Now, whole procedures are finished.

In order to verify the performances of the proposed algorithm, we have perform two types of experiments; one uses digitally generated lines with known parameters  $\alpha$  and another uses a needle-type voltage meter. In the first case, pair of two straight lines are generated digitally with predefined slop angles, then sampled with different spátial resolutions and used as target images to measure the angles between two lines using the proposed FHT. For each  $M$ , two cases are experimentally verified; a needle rotation angle  $\phi_{i1}$  is within the range of the accuracy specification or out of the range. In this way it can be shown that the proposed algorithm can inspect meters correctly.

As illustrated in Table 2, for  $M = 256$ , two images are digitally generated, each of them has two straight lines, angles between these two lines are  $45.2^\circ$  and  $45.8^\circ$ , respectively; they are denoted as  $\Phi_i - \Phi_0$  in the third column of Table 2; the tolerance range of the angle is  $45^\circ \pm 0.5^\circ$ .  $\beta_i$  is obtained using the FHT. From Table 2 we can see that when  $\Phi_i - \Phi_0 - \delta(v_i) > \varepsilon = 0.5^\circ$ , i.e., the needle is out of accuracy range, this case has been successfully detected by using images with a resolution  $M = 256$ . Similarly, using larger  $M$  values, higher accuracies have been achieved as indicated in the Table; for  $M = 512$  and  $M = 1024$ ,  $0.2^\circ$  and  $0.1^\circ$  can be detected.

For a voltage meter of an relative accuracy  $4\%$ ,  $\delta_{max} = 80^\circ$ , the  $\varepsilon = 80^\circ \times 4\% = 3.2^\circ$ . If  $M = 32$ , from Eq. (2)  $\varepsilon_0 = 3^\circ$ , it means that using digital images with  $M = 32$ , this meter can be verified correctly. In our experiment we have used  $32 \times 32$  images to inspect this meter successfully.

#### 5. Conclusions

A fast Hough transform has been presented for inspecting the accuracy of needle-type meter gauges with up to  $0.2\%$  relative accuracy. This FHT is based on a shape analysis of the HT surfaces of the difference images for the needle of the instruments to be tested. Analysis indicates that when a needle is at different angles, although the peak positions  $(\rho_0, \alpha_0)$  change, the shape of the surface  $Z(\rho, \alpha)$  around a small neighborhood centered at  $(\rho_0, \alpha_0)$  does not change. Given a threshold ratio  $C_t$ , all points around  $(\rho_0, \alpha_0)$  which satisfy  $Z(\rho, \alpha) \geq Z(\rho_0, \alpha_0)C_t$  constitute a set which has a shape of two identical right triangles, touching at the same acute angle vertex, each triangle rotated  $180^\circ$  from the other about that vertex. If a needle has a length of  $L$  pixels, the lengths of the two base and height of the right triangle are  $\delta\rho_{max} = \frac{3(0.5 - C_t)}{C_t}$ ,  $\delta\alpha_{max} = \frac{57.3}{C_t L}$ . Experiments show that the surface around peaks is a quasi-singly peaked smooth surface. Considering that property of the surfaces, and that the needle is staying around a set of predetermined angles,  $\alpha_k$ , therefore, we can perform the HT only for parameter  $\theta$  within  $\alpha_k \pm \Delta\alpha_{max}$  instead of whole range of  $\alpha$ ,  $0-180^\circ$ . Furthermore, by properly choosing the origin of image coordinates  $(x,y)$  the rotation axle of the needle can be made near the origin of image coordinates, then the HT can be performed only for  $|\rho| < R$ ,  $R$  is in a range of 3-8 pixels, depending on the

only for  $|\rho| < R$ ,  $R$  is in a range of 3-8 pixels, depending on the image sampling rate. Because the parameter range over which to perform HT is greatly reduced, the number of computations to perform HT is less than one thousandth of that required for the common HT. The shape analysis of the surface  $Z(\rho, \alpha)$  around peak positions is useful in other applications as well. For example, it can be used to locate positions of local peaks more efficiently.

By properly choosing the spatial resolution of the digitization,  $M$ , and the HT parameter angular resolution,  $\Delta\alpha$ , meter gauges of different accuracy grades can be automatically inspected. For an example, in order to inspect instruments with 0.2% accuracy, a 512X512 image and  $\Delta\alpha = 0.2^\circ$  should be used. If  $M$  decreases or  $\Delta\alpha$  increases, the computation load is reduced, but the accuracy which can be verified is decreased accordingly.

Acknowledgments

The authors are grateful for the research support of the Science Foundation of Shanxi Province.

Reference

1. M. L. Baird, "GAGESIGHT: A computer vision system for automatic inspection of instrument gauges," in Conf. Rec. 1982 Workshop on industrial applications of Machine Vision, Research Triangle Park, NC, May 1982, pp. 108-111.
2. C. R. Dyer, "Gauge inspection using Hough transforms," IEEE Trans. Pattern Analysis and Machine Intelligence, Vol. PAMI-5, NO.6, Nov. 1983.
3. P. V. Hough, "Method and means for recognizing complex patterns," U.S. Patent 3069654, Dec. 1962
4. Ke-Qing Li, "Applications of Hough transform in object inspection and identification," Thesis, Dept. of Information System and Engineering, Taiyuan University of Technology, July 1988.

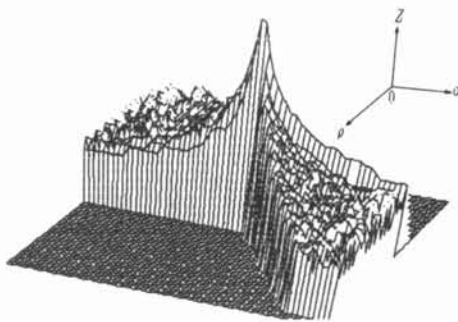


Fig. 4. A 3-D drawing of a peak of the Hough surface.

Table 1.

K	1	2	3	4	5	6	7	8
$H(\rho, \alpha)$	167	145	145	120	86	84	83	64
$\alpha^\circ$	90.0	89.5	90.5	40.0	40.5	91.0	89.0	41.0



Fig. 1. A meter face is digitized with a MxM resolution.

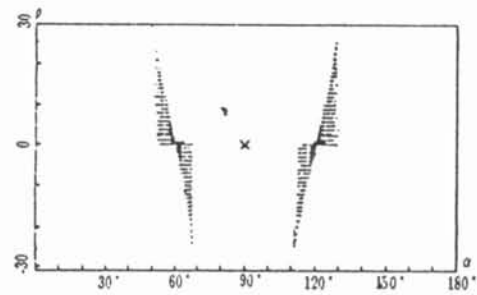


Fig. 2. The printout of the Hough transform amplitude for a  $\Delta I$ , with two lines,  $\alpha = 60^\circ$  and  $120^\circ$ .

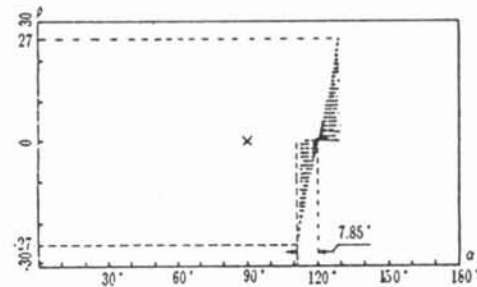


Fig. 3. The printout of the Hough transform amplitude for a  $\Delta I$ , with one line,  $\alpha = 120^\circ$ .

Table 2.

M	$\delta(i) \pm \epsilon$	$\Phi_i - \Phi_0$	$\beta_i$
256	$45.0^\circ \pm 0.5^\circ$	$45.20^\circ$	$45.00^\circ$
		$45.80^\circ$	$46.00^\circ$
512	$75.5^\circ \pm 0.2^\circ$	$75.70^\circ$	$75.60^\circ$
		$75.20^\circ$	$75.20^\circ$
1024	$90.0^\circ \pm 0.1^\circ$	$90.05^\circ$	$90.00^\circ$
		$90.17^\circ$	$90.20^\circ$